A Variance Distribution Model of Surface EMG Signals Based on Inverse Gamma Distribution

Hideaki Hayashi, *Student Member, IEEE,* Junichi Imagi, Yuichi Kurita, *Member, IEEE,* and Toshio Tsuji, *Member, IEEE*

***Abstract*—This paper describes the formulation of a surface electromyogram (EMG) model capable of representing the variance distribution of EMG signals. In the model, EMG signals are handled based on a Gaussian white noise process with a mean of zero. EMG signal variance is taken as a random variable that follows inverse gamma distribution, allowing the representation of noise superimposed onto this variance. Variance distribution is estimated using rectified and smoothed EMG signals, thereby allowing the determination of distribution parameters at low computational cost. A simulation experiment was performed to evaluate the accuracy of distribution estimation using artificially generated EMG signals, with results demonstrating that the proposed model's accuracy is higher than that of maximum likelihood-based estimation. Analysis of variance distribution using real EMG data also suggested a relationship between variance distribution and signal-dependent noise.**

***Index Terms*—Electromyogram (EMG), variance distribution, Bayesian estimation, smoothed and rectified signals, signal-dependent noise.**

I. Introduction

SURFACE electromyogram (EMG) signals, which can be measured from the skin surface, reflect muscular activity. Examples of their application in a wide range of fields, such as rehabilitation, prosthesis control, and motion analysis [1]–[11], include work by Song *et al.* [1], who conducted myoelectrically controlled upper-limb training for post-stroke patients and showed resulting improvement of upper-limb function. Fukuda *et al.* [4] and Shenoy *et al.* [5] also achieved multifunctional prosthesis control using EMG signals measured from multiple electrodes.

In view of the need for appropriate feature extraction in the achievement of these applications, various quantitative evaluation methods for EMG signals have been proposed [12]–[19]. By way of example, frequency domain features such as autoregressive coefficients (AR) [18] and median frequencies (MF) [19] are often used, and their validity for EMG classification has also been demonstrated [9], [10]. However, computation to extract frequency features is time-consuming, and is not always suitable for applications such as prosthesis control where real-time operation is required. In contrast, amplitude features are widely used because of their relatively low computation cost [1]–[8], [11]. The most common methods include rectifying and smoothing processing [12] as seen in the operation of the MyoBock (Otto Bock HealthCare) [11], which is currently the most popular myoelectric hand. In the processing method, the relationship between the processed EMG signal and the corresponding muscle force has been elucidated experimentally [12] but not theoretically.

Meanwhile, Hogan and Mann modeled the relationship between muscle force and raw EMG signals based on Gaussian distribution with a zero mean [15], [16], and hence the muscle force estimation problem can be attributed to the variance estimation problem in raw EMG signals. In the model, however, noise superimposed onto the variance of EMG signals depending on muscle force [20]–[22] cannot be considered because the model estimates variance using the maximum likelihood method under the assumption that variance is constant. The model also has another drawback in that numerous data are required for accurate estimation because the data used in the model are raw EMG signals with a high-frequency component.

This paper proposes a surface EMG model that involves variance distribution in consideration of force-dependent noise based on rectified and smoothed signals and Bayes' theorem. The model estimates variance distribution based on this theorem with EMG variance taken as a random variable, thereby allowing the representation of noise superimposed onto variance depending on muscle force. EMG variance distribution can also be estimated in a small number of samples using rectified and smoothed signals.

The rest of this paper is organized as follows: Section II outlines the structure and estimation method of the proposed model, Sections III and IV detail verification of the model using artificial data and EMG data, respectively, and Section V presents the conclusion.

II. Surface EMG Model

A. Model Structure

Fig. 1 gives an overview of the proposed model, which expresses an EMG signal at t, x_t based on a process involving white Gaussian noise W passed through a shaping filter H and variance σ_t^2, which is the value at t of a random variable σ^2 whose distribution is determined by $\bar{\sigma}^2$ and noise ε depending on muscle force f. The distribution of σ^2 can be estimated using y_t, which is a rectified and smoothed signal of x_t.

First, the relationship between f and $\bar{\sigma}$ can be expressed as follows [15], [16]:

$$\bar{\sigma} = kf^a, \tag{1}$$

H. Hayashi and J. Imagi are with Graduate School of Engineering, Hiroshima University, Higashi-hiroshima, 739-8527 Japan e-mail: (see http://www.bsys.hiroshima-u.ac.jp/).

Y. Kurita and T. Tsuji are with Institute of Engineering, Hiroshima University, Higashi-hiroshima, 739-8527 Japan

Manuscript received April 19, 2005; revised December 27, 2012.

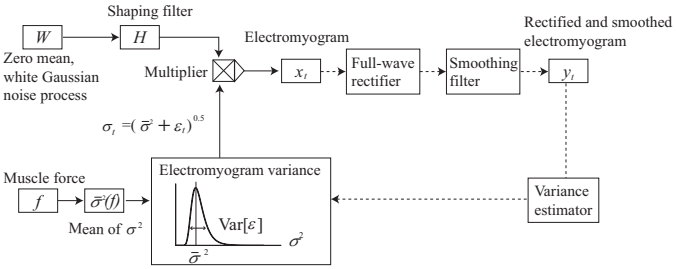

Fig. 1. Overview of the proposed model. The model expresses an EMG signal at t, x_t based on a process involving white Gaussian noise W passed through a shaping filter H and variance σ_t^2, which is the value at t of a random variable σ^2 whose distribution is determined by $\bar{\sigma}^2$ and noise ε depending on muscle force f. The distribution of σ^2 can be estimated using y_t, which is a rectified and smoothed signal of x_t.

where k and a are constants that can be experimentally estimated [15], [16]. σ^2 is then represented by the sum of $\bar{\sigma}^2$ and noise ε.

$$\sigma^2 = \bar{\sigma}^2 + \varepsilon, \tag{2}$$

where ε is a random variable with a zero mean. The mean $E[\sigma^2]$ and the variance $Var[\sigma^2]$ of σ^2 are therefore calculated as

$$\begin{aligned} E[\sigma^2] &= E[\bar{\sigma}^2] + E[\varepsilon] = \bar{\sigma}^2, & (3)\\ Var[\sigma^2] &= E[(\sigma^2 - \bar{\sigma}^2)^2] = Var[\varepsilon]. & (4) \end{aligned}$$

Because x_t is expressed as the multiplication of σ_t and white Gaussian noise W passed through H, x_t obeys Gaussian distribution with a mean of zero and a variance of σ_t^2:

$$P(x_t) = \frac{1}{\sqrt{2\pi\sigma_t^2}} \exp\left[-\frac{x_t^2}{2\sigma_t^2}\right]. \tag{5}$$

y_t is then calculated by rectifying and smoothing x_t using an N-order low pass filter:

$$\begin{aligned} y_t &= a_0 y_{t-1} + a_1 y_{t-2} + \cdots + a_{N-1} y_{t-N} \\ &\quad + b_0|x_t| + b_1|x_{t-1}| + \cdots + b_N|x_{t-N}|, \end{aligned} \tag{6}$$

where $a_0, a_1, \cdots, a_{N-1}$ and $b_0, b_1, \cdots, b_N$ are filter coefficients.

B. Estimation of Variance Distribution

This subsection outlines estimation to determine the distribution of σ^2 using x_t. Given an EMG signal x_t, the posterior distribution of σ^2 $P(\sigma^2|x_t)$ is expressed using Bayes' theorem as follows:

$$P(\sigma^2|x_t) = \frac{P(x_t|\sigma^2)P(\sigma^2)}{P(x_t)}, \tag{7}$$

where $P(x_t|\sigma^2)$ is a likelihood derived from (5) as

$$P(x_t|\sigma^2) = \frac{1}{\sqrt{2\pi\sigma^2}} e^{-\frac{x_t^2}{2\sigma^2}}. \tag{8}$$

Considering that $\sigma^2 > 0$, the inverse gamma distribution $\mathrm{IG}(\alpha, \beta)$ (a conjugate prior for Gaussian distribution) was chosen as the prior distribution $P(\sigma^2)$.

$$P(\sigma^2) = \mathrm{IG}(\sigma^2; \alpha, \beta) = \frac{\beta^\alpha}{\Gamma(\alpha)} (\sigma^2)^{-\alpha-1} e^{\frac{\beta}{\sigma^2}}, \tag{9}$$

where α and β are hyperparameters that determine the inverse gamma distribution and are referred to as the shape parameter and the scale parameter, respectively [23]. The numerator on the right side of (7) is then expanded as follows:

$$\begin{aligned} &P(x_t|\sigma^2)P(\sigma^2) \\ &= \frac{1}{\sqrt{2\pi\sigma^2}} e^{-\frac{x_t^2}{2\sigma^2}} \frac{\beta^\alpha}{\Gamma(\alpha)} (\sigma^2)^{-\alpha-1} e^{\frac{\beta}{\sigma^2}} \\ &= \kappa(\alpha,\beta) \frac{(\beta + \frac{x_t^2}{2})^{(\alpha+\frac{1}{2})}}{\Gamma(\alpha+\frac{1}{2})} (\sigma^2)^{-\alpha-\frac{1}{2}-1} e^{-\frac{\beta+\frac{x_t^2}{2}}{\sigma^2}} \\ &= \kappa(\alpha,\beta) \cdot \mathrm{IG}(\alpha + \frac{1}{2}, \beta + \frac{x_t^2}{2}), \end{aligned} \tag{10}$$

where $\kappa(\alpha, \beta)$ is a constant term described as

$$\kappa(\alpha,\beta) = \frac{\beta^\alpha \Gamma(\alpha+\frac{1}{2})}{\sqrt{2\pi}\Gamma(\alpha)\left(\beta + \frac{x_t^2}{2}\right)^{\alpha+\frac{1}{2}}}. \tag{11}$$

Because $P(x_t)$ and $P(\sigma^2|x_t)$ in (7) must be a constant and a probability density function, respectively, $\kappa(\alpha, \beta)$ and $P(x_t)$ are canceled out, resulting in the correspondence of $P(\sigma^2|x_t)$ with $\mathrm{IG}(\alpha + \frac{1}{2}, \beta + \frac{x_t^2}{2})$. The posterior mean $E[\sigma^2|x_t]$ and the posterior variance $Var[\sigma^2|x_t]$ of σ^2 are then given as follows:

$$E[\sigma^2|x_t] = \frac{\beta + \frac{x_t^2}{2}}{\alpha - \frac{1}{2}}, \tag{12}$$

$$\begin{aligned} Var[\sigma^2|x_t] &= \frac{(\beta + \frac{x_t^2}{2})^2}{(\alpha-\frac{1}{2})^2(\alpha-\frac{3}{2})} \\ &= \frac{(E[\sigma^2|x_t])^2}{(\alpha-\frac{3}{2})}. \end{aligned} \tag{13}$$

From (3) and (4), $E[\sigma^2|x_t]$ and $Var[\sigma^2|x_t]$ correspond to the estimated values of $\bar{\sigma}^2$ and $Var[\varepsilon]$ given x_t, respectively, and $Var[\varepsilon]$ can therefore be estimated from $\bar{\sigma}^2$ by setting α in advance. The next subsection outlines the method used to estimate $\bar{\sigma}^2$ using only a rectified and smoothed signal y_t.

C. Estimation of $\bar{\sigma}^2$

The expectation of y_t is first considered. As this value is given in (6), it is derived as follows:

$$\begin{aligned} E[y_t] &= a_0 E[y_{t-1}] + a_1 E[y_{t-2}] + \cdots + a_{N-1} E[y_{t-N}] \\ &\quad + b_0 E[|x_t|] + b_1 E[|x_{t-1}|] + \cdots + b_N E[|x_{t-N}|], \end{aligned} \tag{14}$$

$E[|x_t|]$ can be calculated with the following formula because x_t obeys the distribution in (5):

$$\begin{aligned} E[|x_t|] &= \int_{-\infty}^{\infty} |x_t| \frac{1}{\sqrt{2\pi\sigma_t^2}} \exp\left[-\frac{x_t^2}{2\sigma_t^2}\right] dx \\ &= \sqrt{\frac{2\sigma_t^2}{\pi}} \\ &= \sqrt{\frac{2}{\pi}(\bar{\sigma}^2 + \varepsilon_t)} \\ &\simeq \sqrt{\frac{2}{\pi}}\left(\bar{\sigma} + \frac{1}{2}\frac{\varepsilon_t}{\bar{\sigma}}\right), \end{aligned} \tag{15}$$

where ε_t is the value of ε at t. Assuming that $E[y_t]$ is temporally stable, (14) and (15) give the following equation:

$$\frac{1-\sum_{i=1}^{N-1} a_i}{\sum_{i=0}^{N} b_i}\sqrt{\frac{\pi}{2}}E[y_t] = \bar{\sigma} + \frac{1}{2\bar{\sigma}}\frac{\sum_{i=0}^{N} b_i \varepsilon_{t-i}}{\sum_{i=0}^{N} b_i}. \quad (16)$$

In (16), the second term on the right-hand side is sufficiently smaller than the first term to be ignored because it has a weighted average of ε_t ($\ll \bar{\sigma}$) based on b_i (> 0) and its expectation is 0. Using (16), $\bar{\sigma}^2$ can therefore be estimated as follows:

$$\bar{\sigma}^2 = \left(\frac{1-\sum_{i=1}^{N} a_i}{\sum_{i=0}^{N} b_i}\right)^2 \frac{\pi}{2} E\left[y_t\right]^2, \quad (17)$$

where the fractional term on the right-hand side corresponds to the reciprocal of the filter gain. As stated above, $\bar{\sigma}^2$ and $Var[\varepsilon]$ can be estimated using the rectified and smoothed signal y_t and the shape parameter α based on (13) and (17) . Note that the raw EMG signal x_t is not required anymore in this estimation.

III. Simulation

A. Method

To evaluate the accuracy of the proposed model for the estimation of variance distribution, simulation experiments were conducted. Artificially generated EMG signals with variance featuring noise superimposed were first generated in line with the following procedures:

(1) A discrete series $\{\sigma_t^2; t = 1, \cdots, T\}$ was generated using random numbers that obey IG(α_0, β_0).
(2) A normal random number that obeys $\mathcal{N}(0, \sigma_t^2)$ was generated for each t and defined as $\{x_t\}$.
(3) $\{x_t\}$ values were regarded as EMG signals measured at a sampling frequency of $F_{\rm s}$ [Hz].

True values for the average of variance and the variance of variance were then given as

$$\bar{\sigma}_0^2 = \frac{\beta_0}{\alpha_0 - 1}, \quad (18)$$

$$Var[\varepsilon_0] = \frac{\beta_0^2}{(\alpha_0-1)^2(\alpha_0-2)}. \quad (19)$$

Accuracy in distribution estimation was verified by comparing these true values with $\bar{\sigma}^2$ and $Var[\varepsilon]$ estimated using the proposed model.

The estimation of $\bar{\sigma}^2$ was conducted using the initial L [ms] of signals $\{y_t\}$ down-sampled at $F_{\rm down}$ [Hz], where $\{y_t\}$ represents rectified and smoothed signals of $\{x_t\}$. Percentage errors between $\bar{\sigma}_0^2$ and $\bar{\sigma}^2$ were then calculated by varying $F_{\rm down}$ as 500, 100, 50, 20, and 10 [Hz] for a fixed value of $L = 1000$ [ms], and varying L as 1000, 500, 200, 100, 50, and 10 [ms] for a fixed value of $F_{\rm down} = 1000$ [Hz]. The results were also compared with those of maximum likelihood estimators for variance calculated using $\{x_t\}$.

In the verification of accuracy for the estimation of $Var[\varepsilon]$, percentage errors between $Var[\varepsilon]$ and $Var[\varepsilon_0]$ were calculated by varying $F_{\rm down}$ as 1000 and 50 [Hz] for a fixed value of $L = 1000$ [ms], and were then compared with those of the variance of variance based on maximum likelihood estimation. This is the variance of K maximum-likelihood variance estimators calculated by dividing L [ms] of $\{x_t\}$ into K equal parts and estimating the variance for each part. The hyperparameters of the prior distribution were determined based on the empirical Bayes method [24], [25] (see Appendix).

Values of $T = 1000$ and $F_{\rm s} = 1000$ were set in each experiment, and a second-order Butterworth low-pass filter (cut-off frequency: 1 [Hz]) was used in smoothing processing. Average percentage errors were calculated by changing the true values 20 times ($\alpha = 15, \beta = 0.5, 1, 1.5, \ldots, 10$).

B. Results

Fig. 2 shows examples of the time-series waveforms of σ_t^2, x_t and y_t, where the data generation parameter β_0 is set as (a) $\beta_0 = 1$, (b) $\beta_0 = 5$, and (c) $\beta_0 = 10$. The vertical and horizontal axes indicate the value of each signal and time, respectively. Fig. 3 shows accuracy in the estimation of $\bar{\sigma}^2$ for each $F_{\rm down}$. The average error rates for the proposed model were: 500 [Hz]: 4.3 ± 2.9 [%]; 200 [Hz]: 4.3 ± 2.9 [%]; 100 [Hz]: 4.3 ± 2.9 [%]; 50 [Hz]: 4.2 ± 2.9 [%]; 20 [Hz]: 4.2 ± 2.9 [%]; and 10 [Hz]: 4.1 ± 2.8 [%]. Those for maximum likelihood estimation were: 500 [Hz]: 3.9 ± 3.0 [%]; 200 [Hz]: 7.5 ± 5.8 [%]; 100 [Hz]: 10.6 ± 6.5 [%]; 50 [Hz]: 15.1 ± 11.2 [%]; 20 [Hz]: 24.9 ± 17.9 [%]; and 10 [Hz]: 30.7 ± 22.1 [%]. Significant differences were observed based on the t-test when $F_{\rm down}$ was 200 or less. Fig. 4 shows the results for each value of L. The average error rates for the proposed model were: 1000 [ms]: 4.3 ± 2.9 [%]; 500 [ms]: 5.1 ± 3.3 [%]; 200 [ms]: 6.4 ± 4.6 [%]; 100 [ms]: 6.5 ± 4.4 [%]; 50 [ms]: 6.5 ± 4.2 [%]; 20 [ms]: 6.4 ± 4.1 [%]; and 10 [ms]: 6.5 ± 4.1 [%]. Those for maximum likelihood estimation were: 1000 [ms]: 3.2 ± 3.0 [%]; 500 [ms]: 4.7 ± 3.3 [%]; 200 [ms]: 9.2 ± 4.7 [%]; 100 [ms]: 12.1 ± 8.8 [%]; 50 [ms]: 18.8 ± 12.5 [%]; 20 [ms]: 21.2 ± 17.2 [%]; and 10 [ms]: 34.8 ± 20.8 [%]. Significant differences were observed based on the t-test when L was 100 or less.

Fig. 5 shows accuracy in the estimation of $Var[\varepsilon]$. When $F_{\rm down} = 1000$, the average error rate for the proposed model was 7.8 ± 5.9 [%], and the error rates for the maximum likelihood method were: $K = 25$: 34.7 ± 16.1 [%]; $K = 10$: 72.6 ± 14.5 [%]; $K = 5$: 88.5 ± 10.0 [%]; and $K = 2$: 96.3 ± 5.12 [%]. When $F_{\rm down} = 50$, the average error rate for the proposed model was 8.0 ± 5.9 [%], and the error rates for the maximum likelihood method were: $K = 25$: 499.4 ± 233.1 [%], $K = 10$: 314.7 ± 300.5 [%], $K = 5$: 247.7 ± 369.1 [%], and $K = 2$: 109.6 ± 150.5 [%]. Significant differences were observed between the outcomes of the proposed model and the maximum likelihood method based on the Bonferroni multiple comparison test.

C. Discussion

Fig. 2 shows that the average and variance of σ_t^2 increase as β_0 increases. The amplitude of x_t and the value of y_t also increase as σ_t^2 increases. Hence, artificial EMG signals with variance where noise is superimposed appear to be generated.

Fig. 3 shows equally high accuracy for the proposed model and the maximum likelihood method when the sampling

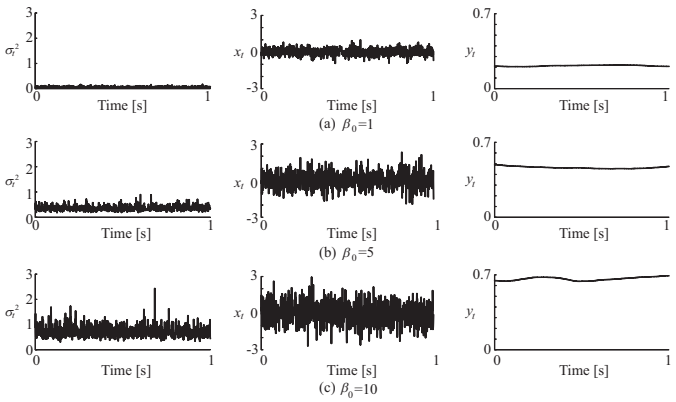

Fig. 2. Examples of σ_t^2, x_t and y_t. σ_t^2 is generated as a random number that obeys IG(α_0, β_0), x_t is a normal random number obeying $\mathcal{N}(0, \sigma_t^2)$ at each t, and y_t is the rectified and smoothed signal of x_t. The data generation parameter β_0 is set as (a) $\beta_0 = 1$, (b) $\beta_0 = 5$, and (c) $\beta_0 = 10$.

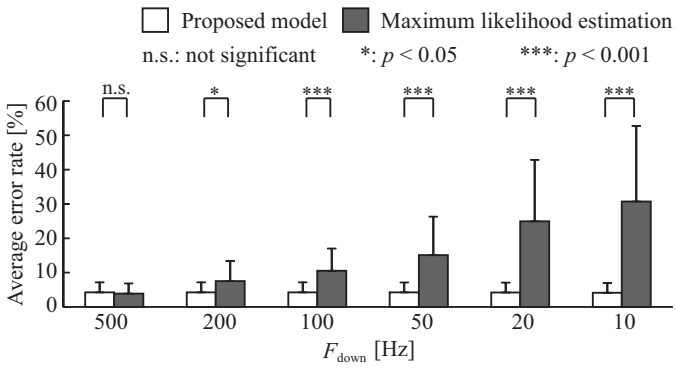

Fig. 3. Average error rate in estimation of $\bar{\sigma}$ for each down-sampling frequency F_{down}

frequency F_{down} was high. The accuracy of the maximum likelihood method, however, decreased as F_{down} decreased, whereas the proposed model maintained high accuracy with an error rate of less than 5 [%]. Although the accuracy of both methods decreased with lower values of L as shown in Fig. 4, the average error rate for the proposed model was about 5 [%] even at $L = 10$ [ms], and was significantly lower than that of the maximum likelihood method. These results show that the proposed model can be used to estimate $\bar{\sigma}^2$ with a small number of samples.

Fig. 5 shows that the average error rates for the proposed model were significantly lower than those for the maximum likelihood. This is because the maximum likelihood method involves the assumption that variance is constant in each division, and cannot sufficiently express the noise superimposed onto variance independently at each time. In contrast, the proposed model involves the assumption that variance is independent at each time, and estimates the posterior distribution of their population. Accordingly, the variance of variance can be estimated with an average error rate of less than about 10 [%].

These results indicate that the proposed model can be used to estimate the variance distribution of EMG signals.

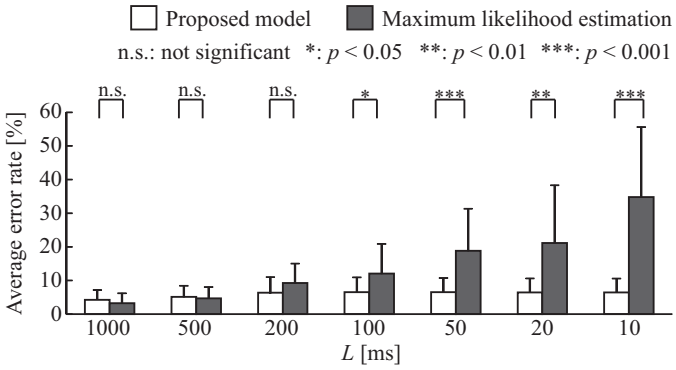

Fig. 4. Average error rate in estimation of $\bar{\sigma}$ for each window width L

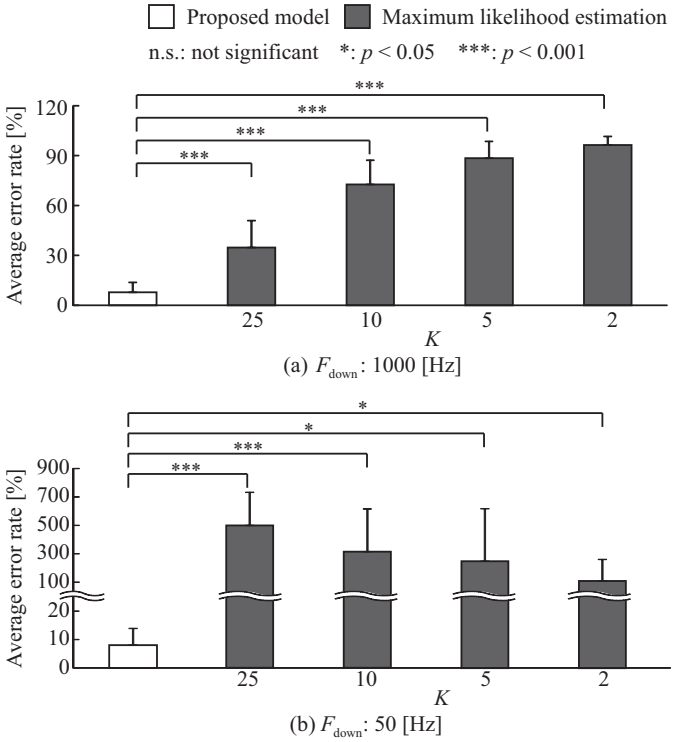

Fig. 5. Average error rate in estimation of $Var[\varepsilon]$ for each down-sampling frequency F_{down} and the number of divisions K. The vertical axis scale from 20 to 100 is omitted in (b).

IV. EMG Analysis

A. Method

To investigate the effectiveness of the proposed model for real biological data, estimation experiments regarding poster distribution $P(\sigma^2|x)$ were conducted. For EMG signal recording, five right-handed subjects (average age: 23.2 ± 0.8) were seated, with the right upper arm pointing downward, the right lower arm bent forward to the horizontal, and the palm turned upward (Fig. 6). EMG signals were recorded from a pair of Ag/AgCl electrodes attached to the biceps brachii at a sampling frequency of 1000 [Hz] while the subjects were weighted with a load on the right wrist and maintained position for 10 seconds with the elbow on a desk (Fig. 6). The load weight was changed through values of 500, 1000, 1500, and 2000 [g], and five trials were conducted for each load weight.

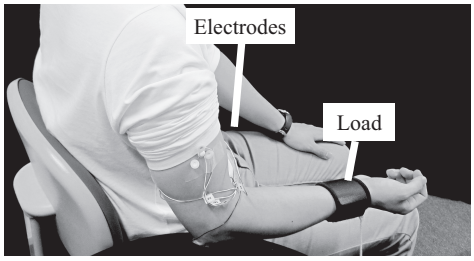

Fig. 6. EMG recording set-up. The subjects were seated with the right upper arm pointing downward, the right forearm bent forward to the horizontal and the palm turned upward. EMG signals were recorded from a pair of electrodes attached to the biceps brachii while the subjects were weighted with a load on the right wrist and maintained position with the elbow on a desk.

A multi-telemeter system (NIHON KOHDEN, WEB-5000, high-frequency cutoff: 100 [Hz], low-frequency cutoff: 5.3 [Hz]) was used for measurement. All subjects were told the aim of the experiment and gave informed consent prior to the trials.

The latter five-second part of the ten seconds of recorded data was used for EMG analysis. The muscle force of the biceps brachii was also calculated assuming that the ratio of forearm/hand weight to body weight was 0.022 [26], the ratio of the length from the elbow to the center of gravity to the length of the forearm/hand was 0.318 [26], and the moment arm length of the biceps brachii to the rotational center of the elbow was 0.03 [m] [27].

Prior distribution hyperparameters were estimated using the empirical Bayes method [24], [25] with single-trial EMG signals recorded in advance under a 2000 [g] load.

B. Results and Discussion

Fig. 7 shows examples of raw EMG signals and rectified and smoothed signals for different load weights of (a) 500 [g], (b) 1000 [g], (c) 1500 [g], and (d) 2000 [g]. The panels of the left show raw EMG signals, and those on the right show rectified and smoothed signals. Fig. 8 shows the posterior distributions of variance $P(\sigma^2|x)$ in a trial, with the distributions of all load weights shown overlapping for each subject. Fig. 9 summarizes the posterior mean $E[\sigma^2|x]$ and the posterior variance $Var[\sigma^2|x]$ of all the trials, and also shows statistical test results based on the Steel-Dwass method. Significant increases in the posterior mean and posterior variance with increased muscle force are seen in four out of the five subjects.

In Fig. 8, the posterior distributions $P(\sigma^2|x)$ shift to the right and spread horizontally as the load weight increases. Accordingly, the posterior mean and posterior variance tend to increase with greater load weights. Fig. 9 indicates that the relationship between muscle force and the posterior mean $E[\sigma^2|x]$ can be expressed in (1) because of their monotonic increasing relationship. Subsequent calculation to determine the values of the exponent a in (1) gave $a = 1.18$, 0.56, 0.81, 0.74, and 0.65 in order of the subjects. Meanwhile, the values of a calculated using the values of σ^2 based on maximum likelihood estimation (as per Hogan and Mann [15], [16]) were $a = 1.17$, 0.55, 0.78, 0.73, and 0.65. These results suggest that the posterior mean $E[\sigma^2|x]$ calculated

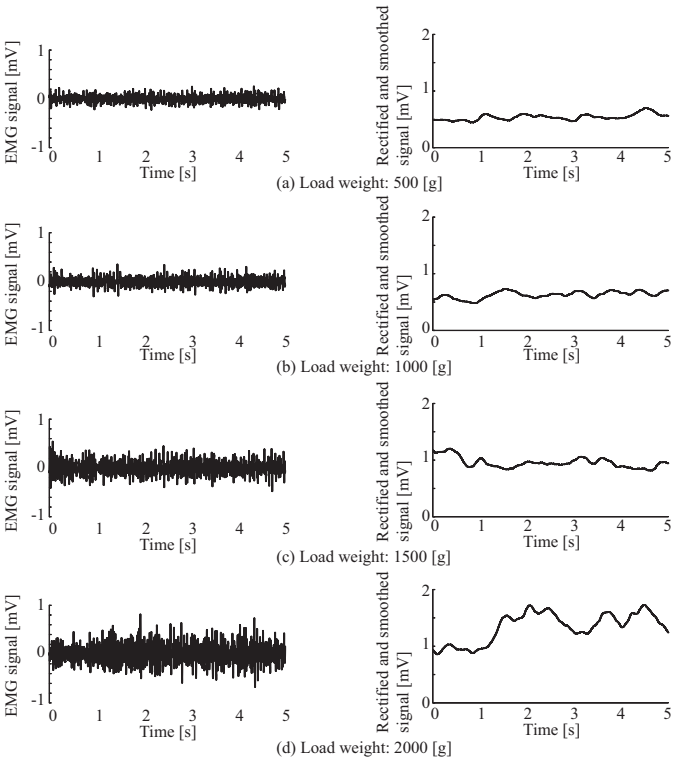

Fig. 7. Examples of EMG signals and rectified/smoothed signals (Subject A). The panels on the left show EMG signals, and those on the right show rectified/smoothed signals.

using the proposed method acts in the same way as variance estimated using the maximum likelihood approach of Hogan and Mann. The remarkable characteristic of the posterior variance $Var[\sigma^2|x]$ is its proportionality to the square of the posterior mean $E[\sigma^2|x]$ in the proposed model, although its increase with greater muscle force is obvious from the increase of $E[\sigma^2|x]$ and (13). Jones *et al.* [21] experimentally showed that the variance of force is proportional to the square of mean force during isometric contraction. The proposed model demonstrates that a similar relationship can be established in the variance of EMG. This means that noise derived from signal-dependent noise is also superimposed onto the variance of EMG signals.

These results indicate that the proposed model can be used to estimate the distribution of variance in EMG signals, and can express noise superimposed onto variance.

V. CONCLUSION

This paper proposed a surface EMG signal model that incorporates variance distribution in consideration of force-dependent noise. The proposed model is used to determine the posterior distribution of variance in EMG signals based on Bayesian estimation, thereby allowing the expression of noise superimposed onto variance depending on force. Posterior distribution can also be estimated from a small number of samples using rectified and smoothed signals.

Simulation using artificial EMG signals revealed that the proposed method can be used to estimate the mean of variance and the variance of variance using a small number of samples

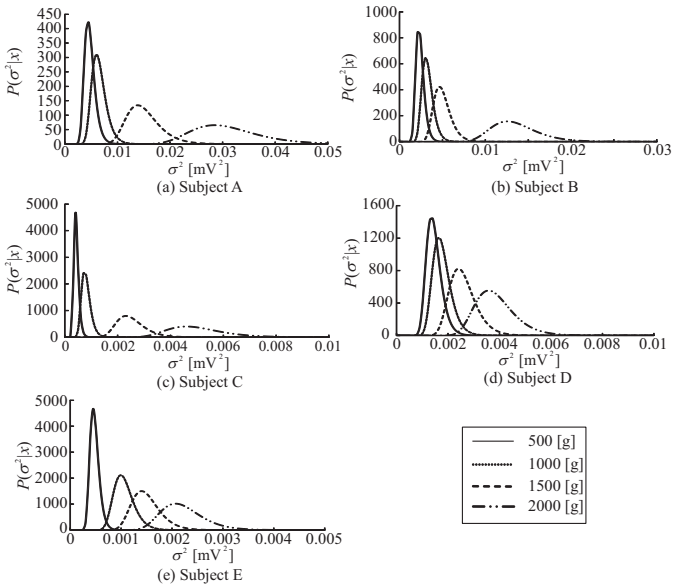

Fig. 8. Examples of posterior distribution $P(\sigma^2|x)$. The distributions of all load weights are shown overlapping for each subject.

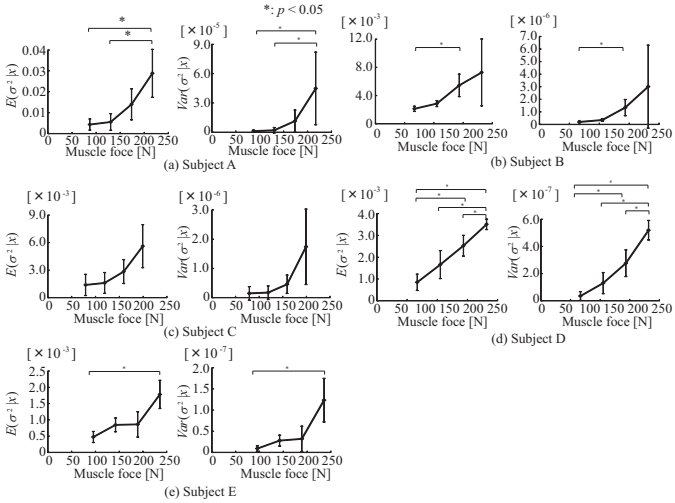

Fig. 9. Posterior mean $E[\sigma^2|x]$ and posterior variance $Var[\sigma^2|x]$ for each muscle force. The panels on the left show the posterior mean $E[\sigma^2|x]$, and those on the right show posterior variance $Var[\sigma^2|x]$.

with a certain level of accuracy. Estimation of the posterior distribution of variance in EMG signals recorded from five subjects also indicated that the variance of variance increased as force increased, which corresponds to the trend previously reported regarding the variance of muscle force [21]. This indicates that the proposed model enables the expression of noise superimposed onto variance.

In future research, we plan to apply the proposed model to EMG pattern classification and muscle force estimation.

APPENDIX
HYPERPARAMETER ESTIMATION FOR PRIOR DISTRIBUTION

The empirical Bayes method [24], [25] allows estimation of hyperparameters for prior distribution from observation. The hyperparameters where observations are most likely to occur are estimated by maximizing the marginal likelihood. This paper refers to the hyperparameter estimation method proposed in (9)

Given n samples of EMG signals $\boldsymbol{x}_n = [x_1, x_2, \cdots, x_n]$, the marginal likelihood $P(\boldsymbol{x}_n|\alpha,\beta)$ of $\boldsymbol{x}_n$ can be expanded as follows:

$$\begin{aligned} P(\boldsymbol{x}_n|\alpha,\beta) &= \prod_{i=1}^{n} P(x_i|\alpha,\beta) \\ &= \prod_{i=1}^{n} \int_{\sigma_i^2} P(x_i|\sigma_i) P(\sigma_i|\alpha,\beta) d\sigma_i^2 \\ &= \prod_{i=1}^{n} \left\{ \frac{\beta^\alpha \Gamma(\alpha+\frac{1}{2})}{\sqrt{2\pi}\Gamma(\alpha)\left(\beta+\frac{x_i^2}{2}\right)^{\alpha+\frac{1}{2}}} \right\} \\ &\quad \times \int_{\sigma_1^2} P(x_1|\sigma_1) P(\sigma_1|\alpha,\beta) d\sigma_1^2 \\ &\quad \cdots \int_{\sigma_n^2} P(x_n|\sigma_n) P(\sigma_n|\alpha,\beta) d\sigma_n^2 \\ &= \prod_{i=1}^{n} \left\{ \frac{\beta^\alpha \Gamma(\alpha+\frac{1}{2})}{\sqrt{2\pi}\Gamma(\alpha)\left(\beta+\frac{x_i^2}{2}\right)^{\alpha+\frac{1}{2}}} \right\}. \end{aligned} \quad (20)$$

As the maximization of $P(\boldsymbol{x}_n|\alpha,\beta)$ is equivalent to the minimization of $-\log P(\boldsymbol{x}_n|\alpha,\beta)$, the evaluation function $J(\alpha,\beta,\boldsymbol{x}_n)$ is then defined for minimization as follows:

$$\begin{aligned} J(\alpha,\beta,\boldsymbol{x}_n) &= -\log P(\boldsymbol{x}_n|\alpha,\beta) \\ &= -\sum_{i=1}^{n} \left\{ -\frac{1}{2}\log(2\pi) + \alpha\log\beta - \log\Gamma(\alpha) \right. \\ &\quad \left. + \log\Gamma\left(\alpha+\frac{1}{2}\right) - \left(\alpha+\frac{1}{2}\right)\log\left(\beta+\frac{x_i^2}{2}\right) \right\} \\ &= \frac{n}{2}\log 2\pi - n\alpha\log\beta + n\log\Gamma(\alpha) \\ &\quad - n\log\Gamma\left(\alpha+\frac{1}{2}\right) + \left(\alpha+\frac{1}{2}\right)\sum_{i=1}^{n}\log\left(\beta+\frac{x_i^2}{2}\right). \end{aligned} \quad (21)$$

α and β are then updated from arbitrary initial values using the steepest descent method [28] as:

$$\begin{bmatrix} \alpha^{(r+1)} \\ \beta^{(r+1)} \end{bmatrix} = \eta \begin{bmatrix} \frac{\partial J(\alpha^{(r)},\beta^{(r)},\boldsymbol{x}_n)}{\partial\alpha} \\ \frac{\partial J(\alpha^{(r)},\beta^{(r)},\boldsymbol{x}_n)}{\partial\beta} \end{bmatrix}, \quad (22)$$

where η is the update rate, and $\frac{\partial J}{\partial\alpha}$ and $\frac{\partial J}{\partial\beta}$ are derived as follows:

$$\begin{aligned} \frac{\partial J}{\partial\alpha} &= -n\log\beta + n\Psi(\alpha) - n\Psi\left(\alpha+\frac{1}{2}\right) \\ &\quad + \sum_{i=1} n\log\left(\beta+\frac{x_i^2}{2}\right), \end{aligned} \quad (23)$$

$$\frac{\partial J}{\partial\beta} = -\frac{n\alpha}{\beta} + \left(\alpha+\frac{1}{2}\right)\sum_{i=1}^{n}\frac{1}{\beta+\frac{x_i^2}{2}}, \quad (24)$$

where $\Psi(\alpha)$ is a digamma function.

REFERENCES

[1] R. Song et al., "Assistive control system using continuous myoelectric signal in robot-aided arm training for patients after stroke," *IEEE Trans. Neural Syst. Rehabil. Eng.*, vol. 16, no. 4, pp. 371–379, Aug. 2008.

[2] E. Akdogan et al., "The cybernetic rehabilitation aid: Preliminary results for wrist and elbow motions in healthy subjects," *IEEE Trans. Neural Syst. Rehabil. Eng.*, vol. 20, no. 5, pp. 697–707, Sept. 2012.

[3] S. R. Taal and Y. Sankai, "Exoskeletal spine and shoulders for full body exoskeletons in health care," *Advances in Applied Sci. Research*, vol. 2, no. 6, pp. 270–286, 2011.

[4] O. Fukuda et al., "A human-assisting manipulator teleoperated by emg signals and arm motions," *IEEE Trans. Robot. Autom.*, vol. 19, no. 2, pp. 210–222, Apr. 2003.

[5] P. Shenoy et al., "Online electromyographic control of a robotic prosthesis," *IEEE Trans. Biomed. Eng.*, vol. 55, no. 3, pp. 1128–1135, Mar. 2008.

[6] K. T. Yoo et al., "Motion analysis and emg analysis of the pelvis and lower extremity according to the width variation of the base of support," *J. Int. Academy of Physical Therapy Research*, vol. 3, no. 1, pp. 391–396, 2012.

[7] D. R. Moynes et al., "Electromyography and motion analysis of the upper extremity in sports," *Physical therapy*, vol. 66, no. 12, pp. 1905–1911, 1986.

[8] Z. Ju and H. Liu, "Human hand motion analysis with multisensory information," *Trans. Mechatron.*, vol. 19, no. 2, pp. 456–466, 2014.

[9] R. Boostani and M. H. Moradi, "Evaluation of the forearm emg signal features for the control of a prosthetic hand," *Physiological measurement*, vol. 24, no. 2, p. 309, 2003.

[10] M. Zecca et al., "Control of multifunctional prosthetic hands by processing the electromyographic signal," *Critical Rev. Biomed. Eng.*, vol. 30, no. 4-6, 2002.

[11] Ottobock, "Ottobock - global start," 2015. [Online]. Available: http://www.ottobock.com/

[12] V. T. Inman et al., "Relation of human electromyogram to muscular tension," *Electroencephalography and clinical neurophysiology*, vol. 4, no. 2, pp. 187–194, 1952.

[13] T. Moritani and H. A. DeVries, "Reexamination of the relationship between the surface integrated electromyogram (iemg) and force of isometric contraction." *American J. Physical Medicine & Rehabilitation*, vol. 57, no. 6, pp. 263–277, 1978.

[14] S. Metral and G. Cassar, "Relationship between force and integrated emg activity during voluntary isometric anisotonic contraction," *European J. applied physiology and occupational physiology*, vol. 46, no. 2, pp. 185–198, 1981.

[15] N. Hogan and R. W. Mann, "Myoelectric signal processing: Optimal estimation applied to electromyography-part i: Derivation of the optimal myoprocessor," *IEEE Trans. Biomed. Eng.*, vol. BME-27, no. 7, pp. 382–395, July 1980.

[16] ——, "Myoelectric signal processing: Optimal estimation applied to electromyography-part ii: experimental demonstration of optimal myoprocessor performance," *IEEE Trans. Biomed. Eng.*, vol. BME-27, no. 7, pp. 396–410, July 1980.

[17] E. A. Clancy and N. Hogan, "Probability density of the surface electromyogram and its relation to amplitude detectors," *IEEE Trans. Biomed. Eng.*, vol. 46, no. 6, pp. 730–739, June 1999.

[18] M. Harba and P. Lynn, "Optimizing the acquisition and processing of surface electromyographic signals," *J. biomed. eng.*, vol. 3, no. 2, pp. 100–106, 1981.

[19] A. Mannion and P. Dolan, "The effects of muscle length and force output on the emg power spectrum of the erector spinae," *J. Electromyography and Kinesiology*, vol. 6, no. 3, pp. 159–168, 1996.

[20] C. M. Harris and D. M. Wolpert, "Signal-dependent noise determines motor planning," *Nature*, vol. 394, no. 6695, pp. 780–784, 1998.

[21] K. E. Jones et al., "Sources of signal-dependent noise during isometric force production," *J. neurophysiology*, vol. 88, no. 3, pp. 1533–1544, 2002.

[22] E. Todorov, "Cosine tuning minimizes motor errors," *Neural Computation*, vol. 14, no. 6, pp. 1233–1260, 2002.

[23] V. Witkovskỳ, "Computing the distribution of a linear combination of inverted gamma variables," *Kybernetika*, vol. 37, no. 1, pp. 79–90, 2001.

[24] B. Efron and C. Morris, "Stein's estimation rule and its competitors - an empirical bayes approach," *J. the American Statistical Association*, vol. 68, no. 341, pp. 117–130, 1973.

[25] H. Akaike, "Likelihood and the bayes procedure," *Trabajos de estadística y de investigación operativa*, vol. 31, no. 1, pp. 143–166, 1980.

[26] D. A. Winter, *Biomechanics of human movement*. John Wiley & Sons Inc, 1979.

[27] T. Tsuji et al., "Impedance regulations in musculo-motor control system and the manipulation ability of the end-point," *Trans. of the Soc. of Instrument and Control Engineers*, vol. 24, no. 4, pp. 385–392, 1988, (in Japanese).

[28] H. Feshbach and P. Morse, *Methods of Theoretical Physics, Part I*. McGraw-Hill Book , London, 1953.

PLACE PHOTO HERE

Hideaki Hayashi (S' 13) received the B.E. and M.Eng degrees from Hiroshima University, Hiroshima, Japan, in 2012 and 2014, respectively. He is currently a Research Fellow of the Japan Society for the Promotion of Science (DC2). His current research interests focus on pattern recognition, neural networks, and biological signal analysis.

PLACE PHOTO HERE

Junichi Imagi received the B.E. and M.Eng degrees from Hiroshima University, Hiroshima, Japan, in 2013 and 2015, respectively.

PLACE PHOTO HERE

Yuichi Kurita (M' 05) received a B.E. degree from Osaka University, Osaka, Japan in 2000, and M.E. and Ph.D. degrees in information science from Nara Institute of Science and Technology (NAIST), Nara, Japan in 2002 and 2004, respectively. Since 2011, he has joined the Institute of Engineering at Hiroshima University as an Associate Professor of the Biological Systems Engineering Laboratory. His research interests include cognitive physics, human biomechanics, haptics, and medical engineering.

PLACE PHOTO HERE

Toshio Tsuji (A' 88–M' 99) the B.E. degree in industrial engineering, and the M.E. and D.Eng. degrees in systems engineering from Hiroshima University, Hiroshima, Japan, in 1982, 1985, and 1989, respectively. He is currently a Professor in the Department of System Cybernetics, Hiroshima University. His current research interests focus on human-machine interface and computational neural sciences, in particular, biological motor control. Dr. Tsuji won the K. S. Fu Memorial Best Transactions Paper Award of the IEEE Robotics and Automation Society in 2003.